Atmospheric Convergence Feedback in a Simple Model for El Niño*

STEPHEN E. ZEBIAK

Lamont-Doherty Geological Observatory, Palisades, NY 10964

(Manuscript received 15 April 1985, in final form 1 January 1986)

ABSTRACT

A parameterization is developed for the feedback between dynamics and heating associated with moisture convergence in the tropical atmospheric boundary layer. The feedback improves the ability of a simple model to simulate observed anomalies of the tropical atmosphere during El Niño events. In particular, two features of the observations are reproduced by including the feedback process: the smaller scale of atmospheric anomalies as compared to SST anomalies, and the focusing of the anomalies in the vicinity of the mean convergence zones. The principal remaining shortcomings of the model are discussed.

1. Introduction

One of the fundamental questions surrounding the El Niño/Southern Oscillation (ENSO) problem is that of how the atmosphere responds to tropical sea surface temperature (SST) anomalies. This question has been the focus of a number of studies, ranging from GCM experiments (e.g., Rowntree, 1972; Keshavamurty, 1983; Shukla and Wallace, 1983) to much simpler modeling studies (Webster, 1981; Simmons, 1982; Zebiak, 1982; Gill and Rasmusson, 1983). It is remarkable that in many respects the results from very simple linear models which parameterize heating in terms of local SST anomalies agree well with those from GCM models in the equatorial region. For example, in response to an imposed large-scale equatorial SST anomaly, all of the models give large equatorial westerly wind anomalies and equatorward wind anomalies to the north and south, with the opposite pattern in the upper troposphere. These are the most prominent features of the tropical wind field during the mature phase of observed ENSO events.

One of the most conspicuous differences between the simplest models and the more sophisticated ones relates to the horizontal length scales of the predicted response. The simple models give wind anomaly fields which vary on the same scale as the imposed SST anomaly field, whereas the GCM models (and the real atmosphere) typically show a response which is much more spatially confined. During the mature phases of a typical ENSO event, the region of largest wind anomalies generally spans only about 10° of latitude, whereas the SST anomaly pattern spans about 30° of latitude (e.g., see Rasmusson and Carpenter, 1982). Furthermore, as pointed out by Ramage (1977) and others, the region of largest wind and convergence anomalies does not always coincide precisely with that of maximum SST anomaly, in contrast to what the simple models predict.

The discrepancy arises because of the parameterization of atmospheric heating solely in terms of local SST anomalies. In reality, the heating is more directly related to low-level moisture convergence (see Ramage, 1977; Newell et al., 1974; Cornejo-Garrido and Stone, 1977). An anomalous low-level influx of moisture increases the conditional instability of the atmosphere, leading to enhanced convection and latent heat release. Because boundary-layer moisture convergence contributes importantly to the net atmospheric heating, and this convergence depends strongly on the flow field itself, there is an internal feedback process between the atmospheric dynamics and the heating field. This feedback can cause the configuration of the final heating and convergence field to differ from that of the SST field, as is observed. The present paper demonstrates this, using the model of Zebiak (1982; hereafter referred to as Z) and a simplified convergence feedback parameterization. The remainder of the paper is organized as follows: section 2 describes the model; section 3 analyzes the feedback algorithm and presents some idealized calculations that illustrate its effect; section 4 shows some ENSO simulations using the present model and compares them to those of the earlier model. The results are discussed in section 5.

2. The model

The governing dynamical equations describe a linear, steady state circulation with a prescribed tropospheric-scale vertical structure. Rayleigh friction and Newtonian cooling are used. On an equatorial β-plane the equations assume the following nondimensional form (see Z):

$$\epsilon u_a - y v_a/2 = -p_x \tag{1a}$$

$$\epsilon v_a + y v_a/2 = -p_y \tag{1b}$$

$$\epsilon p + (u_a)_x + (v_a)_y = -Q \tag{1c}$$

* Lamont-Doherty Geological Observatory Contribution No. 4013.

where u_a and v_a are the components of surface wind anomaly, p is the surface pressure anomaly, ϵ is the damping coefficient (taken to be the same for momentum and thermal damping), and Q is the specified heating anomaly. In Z, the heating anomaly was parameterized in terms of the local SST anomaly by considering temperature-dependent changes in local evaporation. Linearizing the Clausius–Clapeyron relation about the mean SST led to

$$Q = \alpha(\text{SSTA})(b/T_m^2)\exp(-b/T_m), \tag{2}$$

where SSTA is the SST anomaly, T_m is the specified mean SST (climatological monthly means were used), and α and b are constants ($b \approx 5.4 \times 10^3$).

For the present model, the convergence feedback effect is included in a fashion similar to Webster (1981). His approach was to use an iterative procedure in which the diabatic heating for each iteration depends on the low-level convergence from the previous iteration, with the initial diabatic heating specified. The present scheme differs from that of Webster by including the influence of the mean wind field on the feedback process. A heating anomaly should be expected to grow only if the total wind field is convergent, since only then can there be an anomalous influx of moisture. Consider, for example, an initial heating anomaly which occurs in a region of mean divergence. The heating gives rise to an anomalous wind field which is convergent. However, if the mean divergence is strong enough, the total field remains divergent, and there is no source of moisture to allow additional heating. In contrast, an initial negative heating anomaly in a region of mean convergence induces anomalous flow which is divergent, but if the mean convergence is strong enough, the total remains convergent. The reduction in convergence implies less influx of moisture and less total heating; or equivalently, a negative heating anomaly. Thus the initial anomaly is enhanced. If the mean wind field is ignored, the result is that positive heating anomalies are always enhanced, and negative heating anomalies are never enhanced. It is likely that the modulating effect of the mean convergence is a first-order effect on the feedback process, so it is included in the present scheme.

The heating field at iteration n is determined by the relation

$$Q_{n+1} = \begin{cases} Q_0, & \text{if } (\delta_M + \delta'_n) > 0,\ \delta_M > 0 \quad (3a) \\ Q_0 - \beta(\delta_M + \delta'_n), & \\ \qquad \text{if } (\delta_M + \delta'_n) \leq 0,\ \delta_M > 0 \quad (3b) \\ Q_0 + \beta(\delta_M), & \text{if } (\delta_M + \delta'_n) > 0,\ \delta_M \leq 0 \quad (3c) \\ Q_0 - \beta(\delta'_n), & \text{if } (\delta_M + \delta'_n) \leq 0,\ \delta_M \leq 0, \quad (3d) \end{cases}$$

where Q_0 is the initial prescribed heating, δ_M is the mean divergence, and δ'_n is the anomalous divergence at iteration n [which is determined by solving equations (1) for the heating at iteration n and then computing the divergence]. The parameter β may be regarded as an efficiency factor for the feedback process.

According to (3), if the total wind field is divergent and the mean wind field is divergent (case a), there is no feedback, regardless of the sign or magnitude of the anomalous heating. If the mean wind field is divergent, but the anomalous convergence is large enough to make the total wind field convergent (case b), enhancement occurs in proportion to the amount of total convergence (which is less than the anomalous convergence in this case). If the mean wind field is convergent and there is anomalous divergence which is large enough to make the total wind field divergent (case c), then the feedback occurs only in proportion to the strength of the mean convergence (which is less than the strength of the anomalous divergence in this case). Finally, if the mean wind field is convergent and the total wind field is also convergent (case d), then feedback occurs in proportion to the full strength of the anomalous convergence/divergence. Usually, the strength of the mean convergence/divergence is large compared with anomalies so that the cases of no feedback (a) and full strength feedback (d) apply.

3. Analysis of convergence feedback

We can gain some insight into the model feedback by considering the case of an f-plane centered on the equator, i.e., the nonrotating case. It is possible to show either by computation or by the analysis presented in Z that the feedback is most efficient on the equator. Thus the results concerning amplification and convergence of the scheme for this case can be considered global bounds for the system. [Also, the following considers the case of maximal feedback, i.e., (3d).]

The system under study for $f = 0$ is

$$\epsilon u_a^n = -p_x^n \tag{4a}$$

$$\epsilon v_a^n = -p_y^n \tag{4b}$$

$$\epsilon p^n + (u_a^n)_x + (v_a^n)_y = -\alpha Q_0 + \beta[(u_a^{n-1})_x + (v_a^{n-1})_y], \tag{4c}$$

where the superscript n refers to the nth iteration, and αQ_0 is the prescribed initial heating. Equations (4) can be combined to form the single equation

$$-\nabla^2 p^n + \epsilon^2 p^n = -\epsilon\alpha Q_0 - \beta\nabla^2 p^{n-1}. \tag{5}$$

Writing (5) in terms of Fourier modes which have the form

$$Q_0 = Q\exp[i(kx + ly)], \quad p^n = p_0^n \exp[i(kx + ly)]$$

yields

$$p_0^n = \frac{-\epsilon\alpha Q + \beta(k^2 + l^2)(p_0^{n-1})}{k^2 + l^2 + \epsilon^2}. \tag{6}$$

If the initial heating is not maintained (i.e., α set to zero), the feedback from then onward would give

$$p_0{}^n = \frac{\beta(k^2 + l^2)}{k^2 + l^2 + \epsilon^2} p_0{}^{n-1} \equiv a p_0{}^{n-1}. \quad (7)$$

In (7), the coefficient a varies between 0 and β over the whole range of wavenumbers. The sequence defined by (7) diverges if the ratio of successive elements is larger than 1, and converges to zero if the ratio is less than 1. It follows that if $\beta > 1$ the sequence diverges for at least some wavenumbers, and if $\beta < 1$ the sequence approaches 0 for all wavenumbers. A finite nonzero solution therefore requires $\alpha \neq 0$; in other words, an imposed forcing which is maintained for all iterations.

The sequence (6) can be written in the following form:

$$p_0, p_0(1 + a), p_0(1 + a + a^2), \\ p_0(1 + a + a^2 + a^3), \ldots, \quad (8)$$

where

$$a = \beta(k^2 + l^2)/(k^2 + l^2 + \epsilon^2) \quad (9)$$

$$p_0 = -\epsilon\alpha Q/(k^2 + l^2 + \epsilon^2). \quad (10)$$

For $a < 1$, the sequence converges to

$$p_\infty = p_0/(1 - a) \\ = -\epsilon\alpha Q/[\epsilon^2 + (1 - \beta)(k^2 + l^2)]. \quad (11)$$

For $a \geq 1$ the sequence clearly diverges. Thus, if $\beta > 1$, the procedure does not converge. For $\beta < 1$, it converges and gives an amplification of the pressure anomaly which is largest for small wavenumbers. The final value increases with increasing β, and decreases with increasing ϵ. Using (4a) and (4b), the following relations can be derived for the final amplitudes of the Fourier components of u_a and δ (divergence):

$$|U_{a\infty}| = k|Q|/[\epsilon^2 + (1 - \beta)(k^2 + l^2)] \quad (12)$$

$$\delta_\infty = (k^2 + l^2)|Q|/[\epsilon^2 + (1 - \beta)(k^2 + l^2)]. \quad (13)$$

From (12) it is seen that the final zonal wind anomaly approaches zero for both $k \to 0$ and $(k, l) \to \infty$. It is maximized for an intermediate value of k. The divergence anomaly, on the other hand, amplifies most for small scales, with a maximum value $\sim Q/(1 - \beta)$. Therefore if β has a value close to unity, the final convergence anomaly can be very large for a small-scale forcing.

The feedback effect is illustrated in Figs. 1 and 2. Figures 1a and 1b show the initial wind and divergence fields, respectively, for a prescribed large-scale positive heating anomaly of the form

$$Q_0 = \begin{cases} \cos(\pi x/2L_x)\cos(\pi y/2L_y) \\ \quad \text{for} \quad |x - x_0| \leq L_x, |y - y_0| \leq L_y \\ 0, \quad \text{otherwise,} \end{cases} \quad (14)$$

with $L_x = 4$, $L_y = 4$, and with zero mean divergence (the dimensional scale for x and y is about 10° latitude). The atmosphere parameters β and ϵ have the values 0.75 and 0.30, respectively. Figures 1c and 1d show the same fields after the iteration procedure has converged. The convergence amplifies by a factor of two, and decreases in meridional scale, especially to the west of the heating maximum. The wind field amplifies to a lesser extent, with the largest enhancement at the equator to either side of the heating maximum.

In an analagous calculation with a small-scale forcing ($L_x = L_y = 1$), the result is a smaller net wind field response, but a larger amplification of the initial wind and convergence anomalies, as expected from (12) and (13).

In Fig. 2, the prescribed initial forcing is the same as in Fig. 1, but the mean divergence field has the following form:

$$\delta_M = \begin{cases} -6.0, \; 0.5 < y < 1.5 \\ +2.0, \; y < 0.5, \; y > 1.5. \end{cases} \quad (15)$$

This divergence field corresponds to a mean ITCZ between 5°N and 15°N, with divergence to the north and south (a nondimensional value of 1.0 for δ_M corresponds to a dimensional value of 10^{-6} s^{-1}). Again, $\beta = 0.75$ and $\epsilon = 0.3$. The initial wind and divergence fields are the same as Figs. 1a and 1b. The final wind and divergence fields are shown in Figs. 2a and 2b. In the convergence zone, amplification occurs, and to a greater extent than before because the mean convergence imposes a smaller scale on the heating field. The divergence anomaly amplifies much more than before in the mean convergence zone. This is because a negative heating anomaly is allowed to develop in these regions as long as the total flow remains convergent. Without the mean convergence, a negative heating anomaly does not develop, and anomalous divergence can arise only as a result of the remote response to the positive heating anomaly.

The largest wind anomalies are also found in the mean convergence zone, rather than on the equator as before, and the flow has a northward component across the equator in the heating region. The positioning of the mean convergence off the equator produces a noticeably asymmetric response to a symmetric initial forcing.

4. ENSO simulations

The model was used to simulate ENSO wind anomalies by specifying the SST anomaly field from the composites of Rasmusson and Carpenter (1982, hereafter referred to as RC). Three calculations will be shown. In the notation of RC (i.e., year 0 is the ENSO year), they represent the times August (−1), June (0) and December (0). The model parameters are chosen as in Z: $\epsilon = 0.3$ and $\alpha = 1.6$. The feedback parameter β is taken to be 0.75. Rough estimates for the values

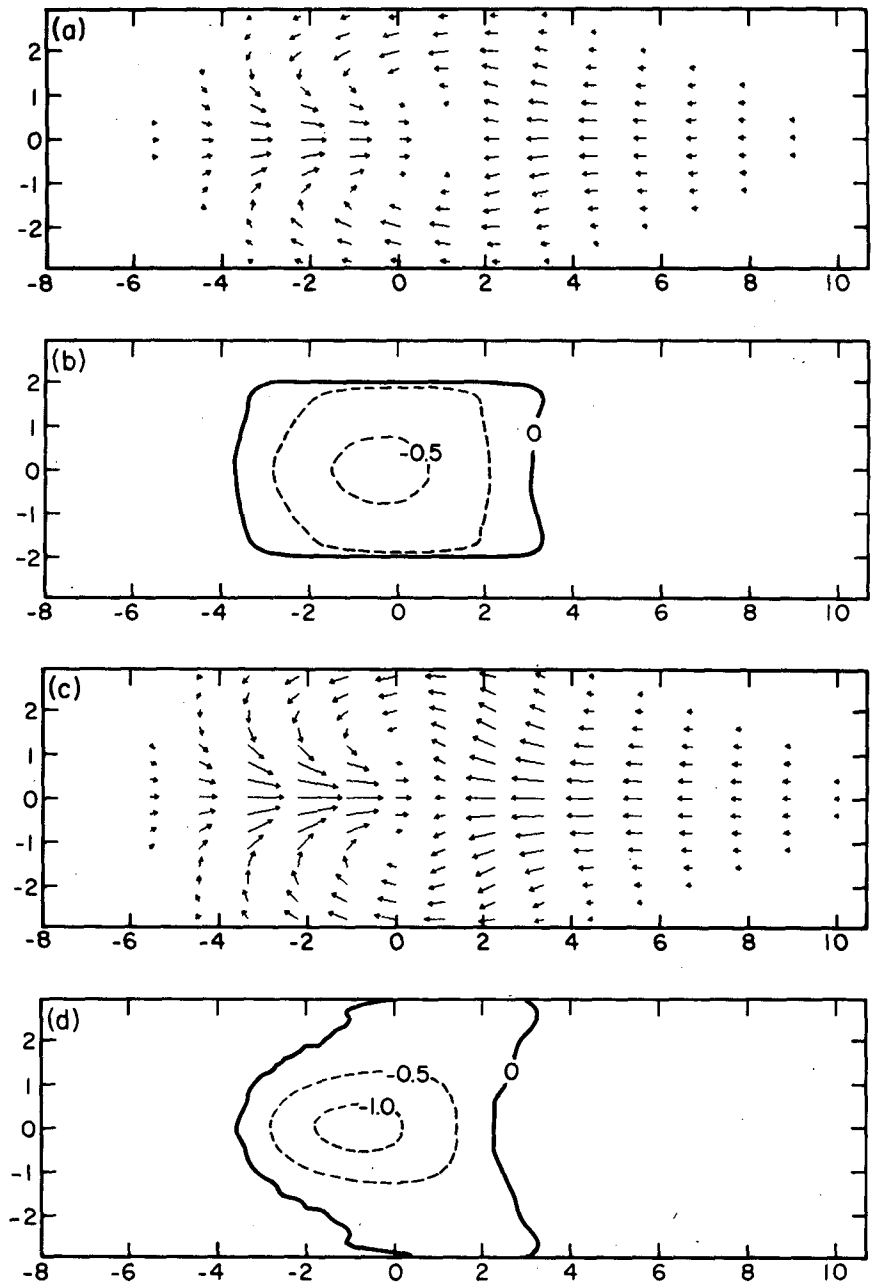

FIG. 1. (a) Initial wind field and (b) initial divergence field for heating of the form $Q = \cos(\pi x/8)\cos(\pi y/8)$. (c) Wind field and (d) divergence field after convergence feedback. Mean divergence field is assumed to be zero.

of α and β can be made by considering a one-dimensional heat balance, and by assuming that the anomalous surface heating is redistributed vertically due to the effect of convection. Such an estimate shows that both α and β should be O(1) (Zebiak, 1984). The present values appear to give the best result within this range. As discussed in Z, the large value of ϵ seems to be essential in this simple model, and probably can be associated only with the net large-scale effects of cumulus convection. This will be discussed further in section 5.

The mean wind fields are specified from the long-term monthly means of RC.

a. August (−1): Pre-event phase

This period is characterized by anomalously cool SST in the central and eastern equatorial regions and

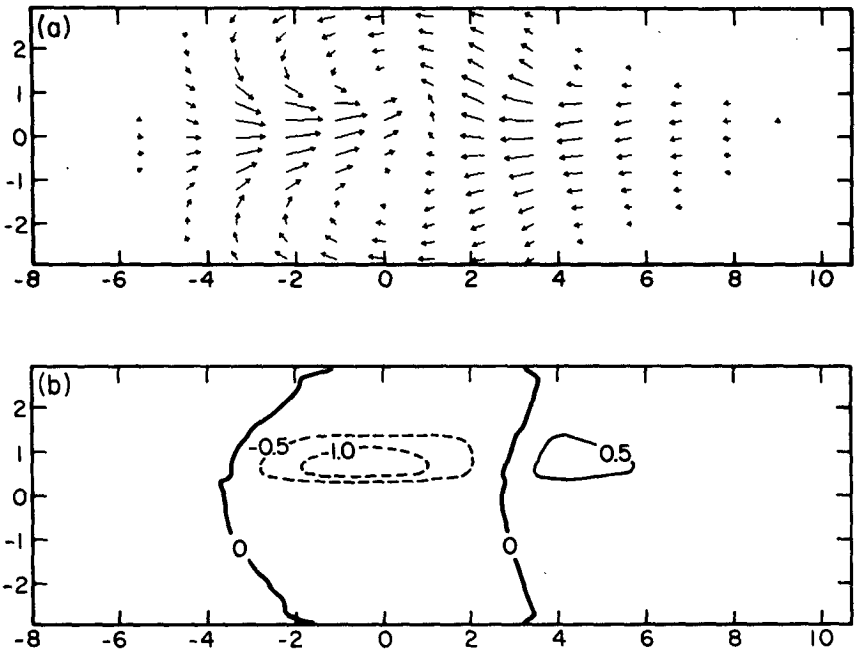

FIG. 2. (a) Wind field and (b) divergence field after convergence feedback, with prescribed mean convergence between $y = 0.5$ and $y = 1.5$, and divergence elsewhere (see text). Initial heating, wind and divergence are the same as for Fig. 1.

anomalously warm SST in the far western equatorial region. Positive SST anomalies also are found on the southern flank of the normal position of the South Pacific Convergence Zone (SPCZ). (See RC for a discussion of such mean features.) Figure 3a shows the composite SST anomaly field for August (−1). Figures 3b and 3e show the composite wind anomaly field and divergence anomaly field for the same time. There are easterly wind anomalies in the western equatorial zone, with poleward flow across the mean positions of the SPCZ and ITCZ in the central Pacific. Correspondingly, there is anomalous divergence between about 10°N and 10°–15°S in the central Pacific, and convergence further poleward. Figures 3c and 3f show the model wind and convergence fields using no feedback (designated model I), and Figs. 3d and 3g show the corresponding fields for the model with convergence feedback (designated model II). The wind fields using models I and II are qualitatively similar, with larger amplitude in the regions of mean convergence in the latter case. Both have easterlies in the same region as does the composite, northerly anomalies across the SPCZ region, and little response in the eastern regions. Looking at the convergence fields, the situation is very different, with much closer agreement with the observations in the case of model II. This is the case in general, and suggests that the low-level convergence field is indeed important in determining a realistic atmospheric heating field. In a number of details, the composite and model II convergence fields differ. However, the details of the computed divergence field for the composite data should be viewed as highly uncertain due to the quality of the data and the averaging and compositing procedures (see RC for a discussion of this). It is only sizable, spatially coherent features that should be considered meaningful for purposes of model comparisons. In this light, the major discrepancy between the model II divergence field and the composite field is the enhanced central Pacific ITCZ which is evident in the composite, and absent in the model results.

b. May (0): Peak phase

Perhaps the most striking oceanic event during ENSO is the rapid and large rise in SST in the eastern Pacific, especially near the South American coast. In the typical event the rise starts in early spring, and SST peaks in May or June. The rise follows by a few months the appearance of sustained westerly wind anomalies in the western and central equatorial Pacific. Figure 4 shows the composite fields and the model I and model II simulations for May (0). There is a local maximum of SST anomaly near the dateline, and larger anomalies extending westward along the equator from the coast. The whole equatorial ocean east of 160°E is warmer than normal by this time. Westerly wind anomalies are present near the dateline and to the west. There is almost no zonal wind anomaly in the eastern regions where the SST anomaly is largest. On the other hand, meridional wind anomalies are large in the vicinity of the ITCZ at this time and are consistent with the ITCZ being displaced southward of its normal position. Poleward of 10°N and 1°S, the eastern Pacific

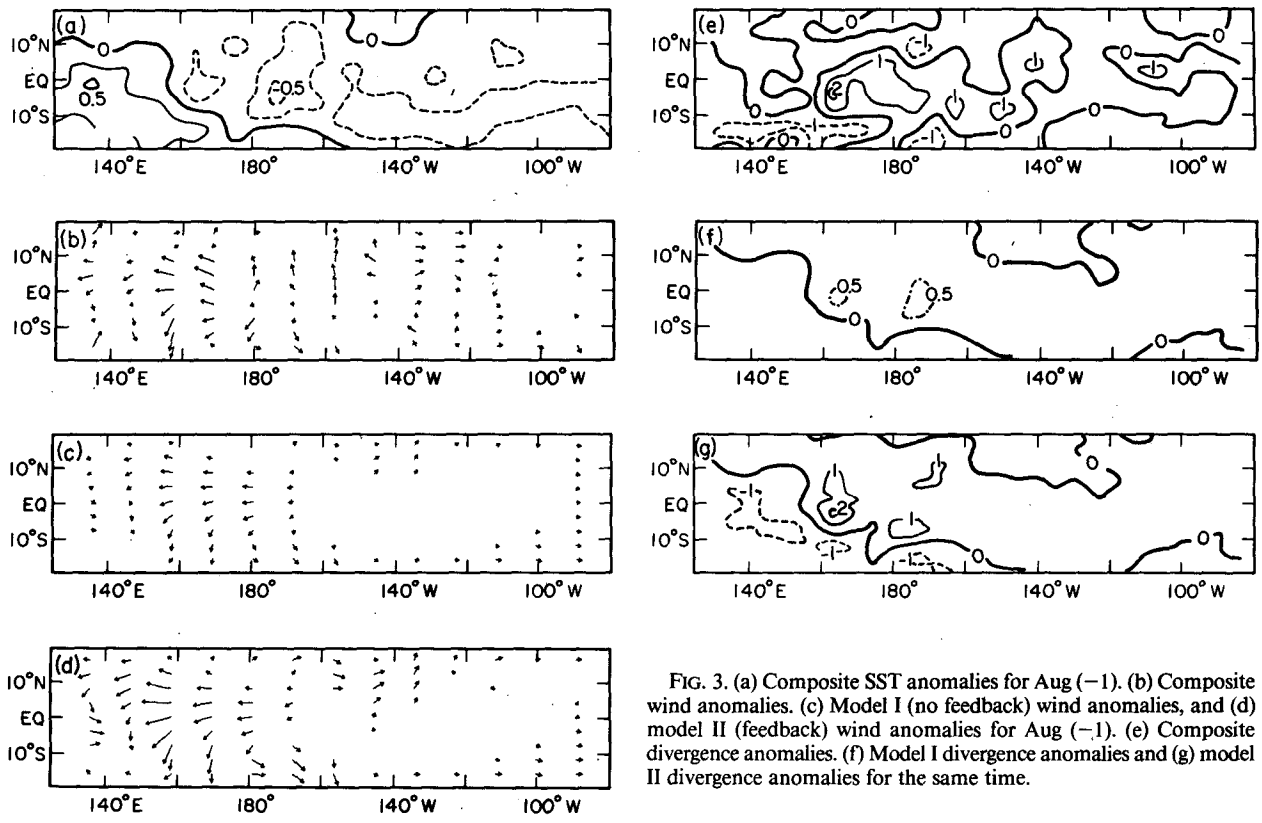

FIG. 3. (a) Composite SST anomalies for Aug (−1). (b) Composite wind anomalies. (c) Model I (no feedback) wind anomalies, and (d) model II (feedback) wind anomalies for Aug (−1). (e) Composite divergence anomalies. (f) Model I divergence anomalies and (g) model II divergence anomalies for the same time.

wind anomalies are small. There is anomalous convergence near the equator in the entire longitude range of warm SST anomalies, with divergence to the north and south. The region of convergence is noticeably smaller in meridional extent than that of the SST anomalies, suggesting that the anomalous heating is so as well.

Although the character of the model I and model II results is the same, the model II results are more comparable to the composites because of the increased relative amplitude of the response near the dateline and in the ITCZ region. The maximum westerly anomalies are displaced slightly to the west of those in the composite. The model wind field near the equator in the east compares favorably with the observations. Away from the equator they differ qualitatively, the model giving substantial easterly anomalies as opposed to the observed weak westerly anomalies.

The model convergence is not as equatorially confined as that of the composite, and the divergence anomalies are weaker. Also the longitudes of maximum convergence differ. However, the two fields basically agree in that they show near-equatorial convergence eastward of 160°E. The differences in the meridional scale of the convergence can be traced to the model heating parameterization which, for example, gives considerable heating at (5°S, 100°W) where apparently there should be none.

c. December (0): Mature phase

Following the coastal peak in SST in May–June, the warm anomalies spread westward so that the central Pacific SST anomaly grows monotonically until December. After June the coastal SST anomaly decreases until September, at which time the maximum SST anomaly is located off the coast at 100°W. Thereafter, the anomalies grow everywhere, but the maximum remains off the coast. This growth follows a significant collapse of the equatorial trade winds in the central Pacific, which occurs in Northern Hemisphere late summer and is sustained until December. This feature is seen in the composite wind anomalies of Fig. 5b. The westerlies are bounded to the north and south by sizeable equatorward winds, reflecting an equatorward displacement of the ITCZ and SPCZ. East of 130°W the anomalous winds are small and directed northward across the equator. Also at this time strong easterly anomalies appear in the western Pacific and are sustained thereafter for several months. The anomalous convergence is large and spans the equatorial central Pacific. It is more equatorially confined than the SST anomalies and centered considerably further to the west.

The region of largest wind anomalies is reproduced very well by model II and less so by model I, the difference between them being primarily in magnitude.

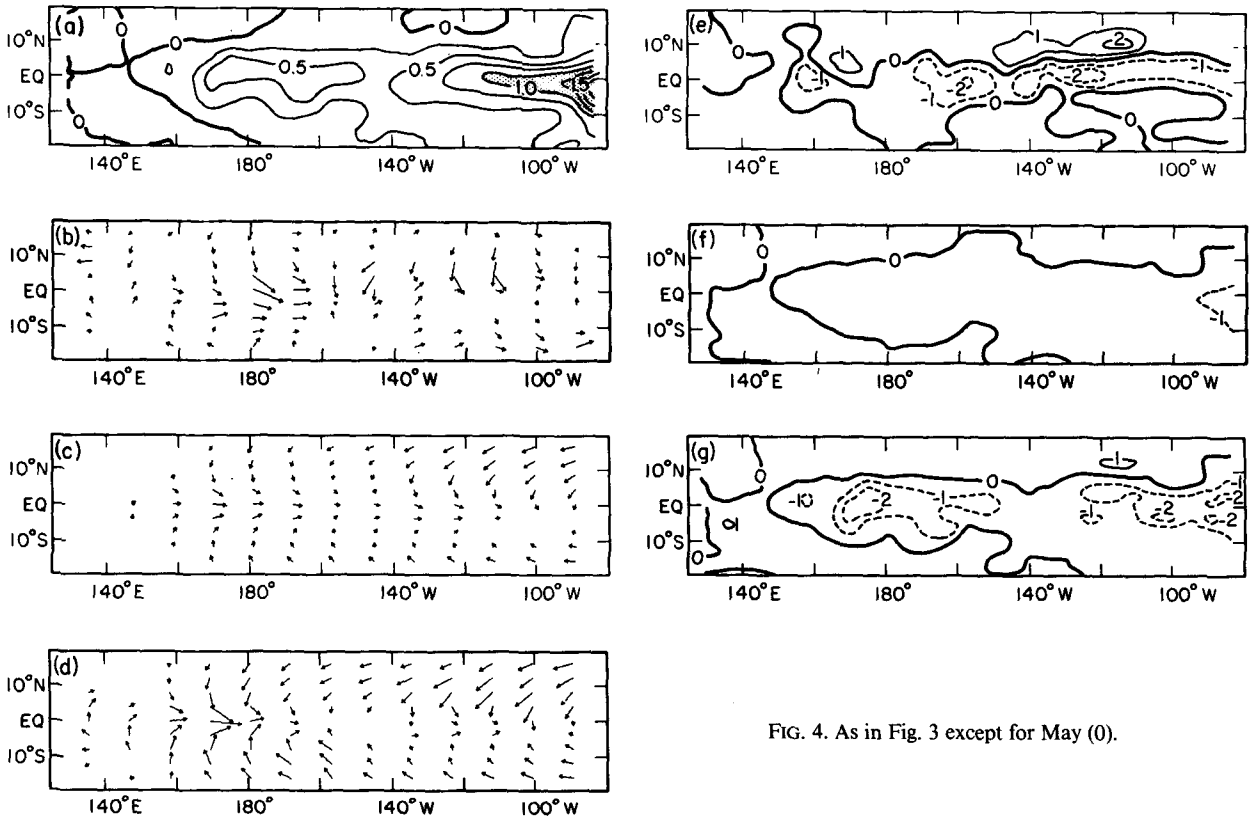

FIG. 4. As in Fig. 3 except for May (0).

In the far west there are discernible easterly anomalies only with model II, and still they are very weak compared with the composite easterlies. In the east, model II gives weak southerlies across the equator as seen in the composite, and model I does not. With either model I or model II, the zonal winds off the equator in the east bear no resemblance to the observations. This cannot be attributed solely to the heating parameterization. Much of the easterly flow in the model arises from the remote response to the large equatorial heating further to the west. The model response to the east of an isolated heat source, attributable to eastward propagating Kelvin waves (Gill, 1980), is characterized by easterly flow of relatively large meridional extent. The Kelvin wave component is most effectively excited by equatorially centered heating of relatively large meridional extent such as that found during the mature phase of ENSO. The composites show no sign of a significant Kelvin wave signal at any time, including the mature phase. It is thus during the mature phase that the disagreement is greatest. Very near the equator the problem is much less serious because the local heating there tends to induce westerly anomalies which partially offset the remotely induced easterly anomalies.

The large difference between the model I and model II convergence shows the degree to which the feedback process can alter the initial heating, both in magnitude and distribution. The effect of the mean convergence zones, especially the SPCZ and ITCZ, are evident. As usual, the model II convergence compares more favorably with the composite. However, while the model II convergence anomalies delineate clearly the normal positions of the mean convergence zones, the composite is more indicative of a movement and/or expansion of the zones. The result is a somewhat different spatial distribution of the convergence anomaly maxima. Specifically, the composite has more equatorial convergence in the central Pacific and less convergence at all latitudes in the far eastern region. In the eastern Pacific ITCZ region, the composite convergence is centered a little closer to the equator, with divergence to the north that is stronger and also equatorward of that in the model. Similar differences are evident at other times as well, but are accentuated in the mature phase when the anomalies are largest.

For the later phases of the event, the model exhibits the same strengths and weaknesses evident in the mature phase. That is, in amplitude and spatial patterns, the model II results compare better with the observations. However both models fail to reproduce the large equatorial easterly anomalies in the western Pacific that persist for nearly a year after the mature phase, and both models produce a large easterly wind response in the eastern part of the basin which is not observed.

5. Summary and discussion

The results show that, by including a simple moisture convergence feedback parameterization, the dynami-

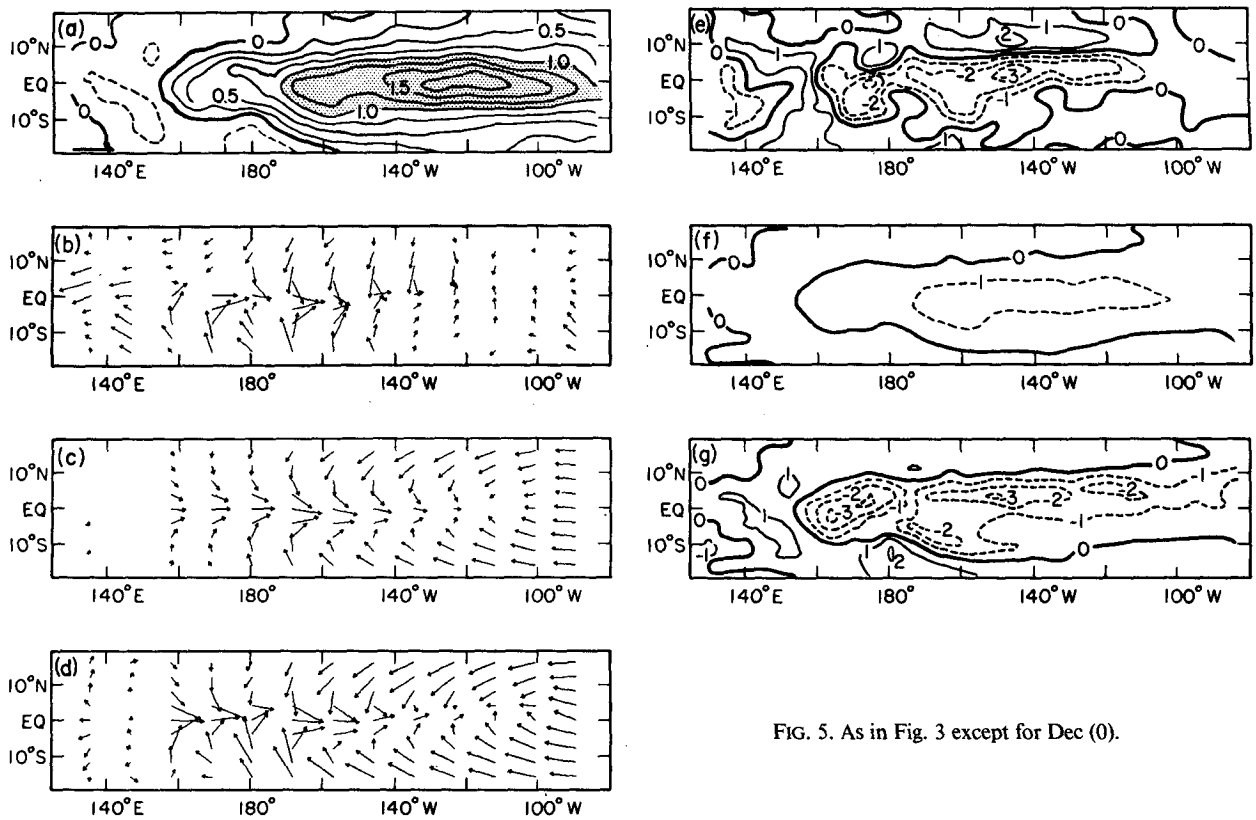

FIG. 5. As in Fig. 3 except for Dec (0).

cally simple model of Zebiak (1982) is considerably improved in its ability to simulate the observed atmospheric anomalies during ENSO. The feedback results in a reduction of scale in the atmospheric response to imposed heating anomalies and provides a plausible explanation for observed difference in scale between typical atmospheric and oceanic anomaly patterns during ENSO. The mean low-level convergence fields, which were specified in these calculations, strongly modulate the feedback process and are largely responsible for the more realistic results.

Despite the improvement, the model still fails to reproduce some of the characteristics of the observations—most notably, the development of equatorial easterlies in the western Pacific during the mature phase of ENSO and thereafter and the absence of significant zonal wind anomalies in the eastern Pacific during all phases of ENSO. Some of this discrepancy may be due to heating anomalies in the South American and Indian Ocean regions which were ignored in this study. However, this is unlikely to be the sole explanation for the differences. Precipitation anomalies in both these regions are considerably smaller than those in the Pacific. In the South American case, the influence is also questionable due to the presence of the Andes. Even without this complication, a model heating anomaly over tropical South America would induce a "Rossby mode" westerly wind response of considerably smaller meridional extent than the "Kelvin mode" easterly response to the east of the large central Pacific heat source.

Further progress may require additional model refinements. For example, the model probably would be improved by including a more complete moisture budget. Among other effects, this would allow for variations in specific humidity associated with the *mean* SST field. Since the dependence of specific humidity is a strongly nonlinear function of temperature, the result would be stronger heating anomalies in the western Pacific (where SST is highest), and much smaller heating anomalies in most of the eastern Pacific. This is what is required, as indicated by the convergence fields of Figs. 4 and 5. It should be noted that the incorporation of a realistic moisture budget may additionally require an explicit model boundary layer.

Another possible model improvement is to allow the model friction to depend on the heating field (i.e., the intensity of convection). It has been argued that the large friction can be justified only by appealing to momentum mixing associated with convection. If this is correct, then the effect should be confined to where moisture convergence and heating are large and absent in regions of divergence, where convection is suppressed. Of course, in order to allow for this variation, the model must be applied to the *total* fields, rather than just the anomaly fields as done here. This modification, though, probably would improve the model

results in the eastern Pacific region. The wind field over most of this region remains divergent even during ENSO events, and thus the parameterization would always give very small friction here. Consequently, there would be little variation in the intensity of the easterlies as a result of the eastward migration of the Indonesian heat source into the central Pacific during ENSO (recall that the response decreases to the east of the heat source with a scale inversely proportional to the friction parameter). The present model (applied to the total fields) gives a large variation in the easterlies because, with the large friction, the longitudinal decay scale of the easterlies is comparable to the distance the heat source moves/expands eastward.

In this study, including the convergence feedback mechanism has been relatively simple and has significantly improved the model. It appears that an even better simulation of the observations is possible with a modest increase in model complexity. This is particularly encouraging for prospects of coupled atmosphere–ocean modeling of ENSO, which requires very lengthy integrations that presently are not feasible with complete general circulation models.

Acknowledgments. My thanks to Dr. Mark Cane for helpful discussions regarding this work and to Karen Streech for the preparation of the manuscript. This work was supported by NASA Grant NAGW-582.

REFERENCES

Cornejo-Garrido, A. G., and P. H. Stone, 1977: On the heat balance of the Walker circulation. *J. Atmos. Sci.*, **34,** 1152–1162.

Gill, A. E., 1980: Some simple solution for heat-induced tropical circulation. *Quart. J. Roy. Meteor. Soc.*, **106,** 447–462.

Keshavamurty, R. N., 1983: Southern Oscillation: Further studies with a GFDL general circulation model. *Mon. Wea. Rev.*, **111,** 1988–1997.

Newell, R. E., J. W. Kidson, D. G. Vincent and G. J. Boer, 1974: *The General Circulation of the Tropical Atmosphere and Interactions with Extra-tropical Latitudes.* MIT Press, 371 pp.

Ramage, C. S., 1977: Sea surface temperature and local weather. *Mon. Wea. Rev.*, **105,** 540–544.

Rasmusson, E. M., and T. H. Carpenter, 1982: Variations in tropical sea surface temperature and surface wind fields associated with the Southern Oscillation/El Niño. *Mon. Wea. Rev.*, **110,** 354–384.

Rowntree, P. R., 1972: The influence of tropical east Pacific Ocean temperatures on the atmosphere. *Quart. J. Roy. Meteor. Soc.*, **98,** 290–321.

Shukla, J., and J. M. Wallace, 1983: Numerical simulation of the atmospheric response to equatorial Pacific sea surface temperature anomalies. *J. Atmos. Sci.*, **40,** 1613–1630.

Simmons, A. J., 1982: The forcing of stationary wave motion by tropical diabatic heating. *Quart. J. Roy. Meteor. Soc.*, **108,** 503–534.

Webster, P. S., 1981: Mechanisms determining the atmospheric response to sea surface temperature anomalies. *J. Atmos. Sci.*, **38,** 554–571.

Zebiak, S. E., 1982: A simple atmospheric model of relevance to El Niño. *J. Atmos. Sci.*, **39,** 2017–2027.

——, 1984: Tropical atmosphere–ocean interaction and the El Niño/Southern Oscillation phenomenon. Ph.D. dissertation, MIT, 261 pp.